Structure
Article

Structure of the PTEN-like Region of Auxilin, a Detector of Clathrin-Coated Vesicle Budding

Rong Guan,[1,4] Dai Han,[2] Stephen C. Harrison,[2,3] and Tomas Kirchhausen[1,4,*]
[1]Department of Cell Biology
[2]Jack and Eileen Connors Structural Biology Laboratory, Department of Biological Chemistry and Molecular Pharmacology
Harvard Medical School, Boston, MA 02115, USA
[3]Howard Hughes Medical Institute, Chevy Chase, MD 20815-6789, USA
[4]Immune Disease Institute and Program in Cellular and Molecular Medicine at Children's Hospital, Boston, MA 02115, USA
*Correspondence: kirchhausen@crystal.harvard.edu
DOI 10.1016/j.str.2010.06.016

SUMMARY

Auxilin, a J-domain containing protein, recruits the Hsc70 uncoating ATPase to newly budded clathrin-coated vesicles. The timing of auxilin arrival determines that uncoating will commence only after the clathrin lattice has fully assembled and after membrane fission is complete. Auxilin has a region resembling PTEN, a PI3P phosphatase. We have determined the crystal structure of this region of bovine auxilin 1; it indeed resembles PTEN closely. A change in the structure of the P loop accounts for the lack of phosphatase activity. Inclusion of phosphatidylinositol phosphates substantially enhances liposome binding by wild-type auxilin, but not by various mutants bearing changes in loops of the C2 domain. Nearly all these mutations also prevent recruitment of auxilin to newly budded coated vesicles. We propose a specific geometry for auxilin association with a membrane bilayer and discuss implications of this model for the mechanism by which auxilin detects separation of a vesicle from its parent membrane.

INTRODUCTION

Clathrin-mediated endocytosis carries a large part of the membrane traffic that originates at the cell surface and terminates at membrane-bound internal compartments. Assembly of a clathrin lattice around an invaginating vesicle engulfs membrane-associated components, including receptors and their bound ligands (Brett and Traub, 2006; Kirchhausen, 2009). Once the vesicle has pinched off from the parent membrane, the coat is lost, and its components are recycled (Lee et al., 2006; Massol et al., 2006). The vesicle itself can then fuse with the membrane of a suitable target compartment. The uncoating step is the point at which ATP hydrolysis drives the cycle of clathrin assembly and disassembly in a unique direction (Barouch et al., 1994; Greene and Eisenberg, 1990; Schmid and Rothman, 1985). The uncoating ATPase is Hsc70, a member of the heat shock protein 70 (Hsp70) family. Like all Hsp70 homologs, Hsc70 has a J-domain containing partner that determines the specificity of its target. In the case of clathrin coats, the relevant J-domain protein is known as auxilin (Ungewickell et al., 1995).

Endocytic clathrin-coated vesicles shed their coats almost immediately after budding from the plasma membrane (Lee et al., 2006; Massol et al., 2006). The timing is determined by the arrival of auxilin, which in turn recruits Hsc70. Recruitment of auxilin only after membrane budding is complete ensures that Hsc70-driven uncoating does not compete with coat assembly (Massol et al., 2006). Mammalian species have two auxilin paralogs: auxilin 1(Ahle and Ungewickell, 1990), which is neuron specific, and auxilin 2, which is ubiquitous. The organization of the auxilin 1 polypeptide chain is shown in Figure 1A. The elements essential for binding clathrin coats and recruiting Hsc70 are in the C-terminal half of the molecule. The N-terminal part has an amino acid sequence that can be aligned with the phosphatase and C2 domains of the phosphoinositide phosphatase, PTEN. Differences at key residues in the catalytic cleft suggest that the PTEN-like region of auxilin will not have phosphatase activity, however, and indeed, no activity can be detected. Auxilin 2, also known as GAK (cyclin G-associated kinase; Kanaoka et al., 1997), has an additional, N-terminal kinase domain.

A fragment of auxilin 1 comprising residues 547–910 supports Hsc70 and ATP-dependent uncoating in vitro as well as does the full-length protein (Holstein et al., 1996). In cells, however, auxilin that lacks the PTEN-like region fails to associate with coated vesicles (Massol et al., 2006). The PTEN-like part of auxilin thus appears to be the detector that reports when the vesicle within the coat has separated from the plasma membrane (Massol et al., 2006). Electron cryomicroscopy (cryoEM) and three-dimensional image reconstruction of clathrin coats with bound auxilin (547–910) show that the clathrin-binding region (residues 550–750, approximately) contacts a surface of the clathrin terminal domain, on the internal face of the clathrin lattice (Fotin et al., 2004). The PTEN-like region would then project inward and presumably contact the lipid vesicle. Because the amino acid sequence of this region implies that it closely resembles a phosphoinositide phosphatase (Haynie and Ponting, 1996), we have proposed that it is likely to recognize a phosphoinositide head group (Massol et al., 2006). We have further suggested that stable recruitment at the concentration of auxilin in a cell requires both the contacts with clathrin seen by cryoEM

A

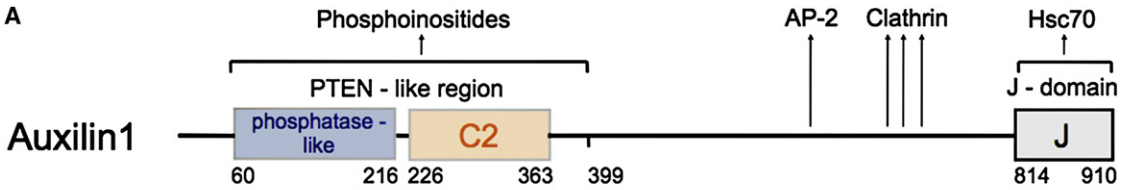

B

Construct	Mutation	Location of Mutation
1	wt	
2	R301E/R307E/K311E	C2 domain loop3
3	R301E/R307E	C2 domain loop3
4	R301E/K311E	C2 domain loop3
5	R307E/K311E	C2 domain loop3
6	R301E	C2 domain loop3
7	R307E	C2 domain loop3
8	K311E	C2 domain loop3
9	I304D/L308D	C2 domain loop3
10	I304D	C2 domain loop3
11	L308D	C2 domain loop3
12	H159A/C160A	Phosphatase-like domain P loop
13	G164A	Phosphatase-like domain P loop
14	K243E/R245E	C2 domain loop1
15	K243E	C2 domain loop1
16	R245E	C2 domain loop1

Figure 1. Domain Organization of Auxilin and Description of Mutants

(A) Domain organization of the neuron-specific auxilin 1, highlighting regions that interact with its most important effector molecules.

(B) List of mutants used in this work for in vitro lipid binding studies of the PTEN-like region of auxilin and for in vivo studies by live-cell imaging.

and a membrane interaction of the PTEN-like domain. If an enzymatic activity that generates the species recognized by that domain is present in the coat, then its product will diffuse rapidly away as long as the vesicle bud remains continuous with the adjacent plasma membrane. As soon as dynamin-driven fission is complete, however, the product will accumulate in the vesicle. One candidate for this postulated enzymatic activity is synaptojanin, a lipid phosphatase that remove the 5-phosphate from PI (4,5) P2 (Perera et al., 2006; Woscholski et al., 1997).

We describe here the structure of the PTEN-like region of auxilin 1, which we have determined to help test the mechanism outlined in the preceding paragraph. The structure is, as expected, nearly identical to that of PTEN (Lee et al., 1999). The ''catalytic cleft,'' although devoid of enzymatic activity, has essentially the same geometry as in PTEN, and it could therefore accommodate an inositol phosphate group. We show that the fragment we have crystallized, auxilin (40–400), binds liposomes containing PI4P and PI (4,5) P2 and that mutations in the C2 domain, in loops known to contact membranes in C2 domains of other proteins, eliminate this binding. We also tested the effects of the mutations on recruitment of full-length auxilin to coated pits, using previously described live-cell imaging methods and found good concordance of lipid-binding and recruitment. We propose a model for the orientation of the protein on a membrane bilayer and discuss its implications for the mechanism by which auxilin detects separation of a vesicle from its parent membrane.

RESULTS AND DISCUSSION

Structure Determination

We expressed a set of nested constructs, spanning the predicted PTEN homology region within the N-terminal half of bovine auxilin 1. We could recover auxilin (1–400) with good yield, but the product showed evidence of proteolytic degradation to a smaller, stable species. Mass spectrometric analysis identified the end product as auxilin (40–400), which we expressed, purified, and crystallized as outlined in Experimental

Table 1. Data Collection and Refinement Statistics

A. Data Collection	
Space group	P3221
Resolution (Å)	50–2.18 (2.22–2.18)
Unit Cell Dimensions	
a, b, c (Å)	137.925, 137.925, 51.327
α, β, γ (°)	90.00, 90.00, 120.00
Completeness	99.9 (99.4)
Rmerge (%)	8.2 (53.1)
I/σ (I)	22.4 (2.6)
Redundancy	7.6 (4.7)
Wilson B factor (Å2)	39.14
B. Refinement	
Resolution (Å)	38.90–2.18
No. of reflections Rwork/Rfree	28,006/1477
Rwork/Rfree (%)	17.19/21.92
Number of solvent molecules	215
Number of $Ca2^+$/Cl^- ions	1 / 2
Average B factor (Å2)	43.75
Rms bond lengths (Å)	0.019
Rms bond angles (°)	1.63

Procedures. The crystals are in space group P3221 (a = b = 137.9, c = 51.3), with a single polypeptide chain per asymmetric unit. We recorded diffraction data to a minimum Bragg spacing of 2.18 Å and determined the structure by molecular replacement with a modified PTEN structure as the search model. Table 1 summarizes the data collection and refinement statistics. The final model contains residues 60–75 and 88–399; the first 20 residues and the loop spanning residues 76–87 are disordered (Figure 2).

Molecular Structure

The molecule has a roughly crescent shaped outline, about 60 × 35 × 35 Å in external dimensions. Just as does PTEN itself (Lee et al., 1999), auxilin (40–399) comprises a phosphatase-like domain (residues 54–216) and a C2 domain (residues 226–363). Residues 363–399 extend back against the phosphatase-like domain, so that the N and C termini of the fragment polypeptide chain are at the same end of the crescent. The interface between the two domains contains both hydrogen-bond networks and a hydrophobic core, so that the orientation of one domain with respect to the other is probably fixed. In PTEN, the interface is also a tight one, and mutations at that interface compromise function.

The structure of the phosphatase-like domain follows very closely that of the PTEN phosphatase domain (rmsd = 1.60 Å for 130 of the 144 ordered alpha carbons between residues 62 and 217), but with some altered active-site residues. The "P loop" (residues 160–167) (Figure 3A) differs in conformation from its PTEN counterpart, so that the tip of the loop covers what would be the active-site cysteine at its base. In auxilin, the HCxxGxxR motif, conserved in P loops of protein tyrosine phosphatases and dual-specificity phosphatases as well as in PTEN and its orthologs, lacks the final arginine, and various other residues believed to participate in substrate recognition or in catalysis are also different (e.g., auxilin Ile129, which corresponds to PTEN Asp92). Nonetheless, except for absence of the cavity presumably occupied by the D3 phosphate of PtdIns-3,4,5-P3, the inactive "catalytic cleft" in auxilin has roughly the same shape as the active cleft in PTEN.

The C2 domain, a sandwich of two, four-stranded, antiparallel β sheets, has a so-called topology II C2 structure and lacks the canonical $Ca2^+$ liganding residues in loops 1 and 3 that characterize those C2 domains dependent on $Ca2^+$ for lipid-binding activity (Sutton et al., 1995; Sutton and Sprang, 1998). Its framework of eight β strands is essentially identical to that of PTEN (rmsd = 1.09 Å for 80 residues between 227 and 364), but the loops deviate more substantially, especially loops β1-β2 and β5-β6, on the surface of the domain that probably faces the membrane. The β5-β6 loop projects away from the body of the domain as an unusually long, somewhat twisted, β hairpin. It contains three positively charged residues, and two exposed hydrophobic side chains project at its tip. In PTEN, there is a disordered loop (β6-β7) on the side of the C2 domain likely to face away from the membrane; this loop, excised when the PTEN structure was determined, is a short, well-ordered turn in auxilin.

Membrane Binding

We examined association of auxilin (40–400) with large, multilamellar PC liposomes containing the negatively charged phospholipids, PS, PI, PI4P and PI (4,5) P2 at 5%, 10%, and 15%, with pure PC liposomes as a control. The liposomes were sedimented and examined by SDS-PAGE (Figure 3B). Only the phosphoinositide-containing liposomes bound the auxilin fragment more strongly than PC alone, with an approximate affinity ranking, PI4p > PI (4,5) P2, in agreement with previous lipid-overlay data (Lee et al., 2006; Massol et al., 2006). We also tested the effects of mutations in loops 1 (β1- β2) and 3 (β5-β6) of the C2 domain, likely from studies of other C2 domains to be important membrane contacts (Bai et al., 2004) (Figures 1B and 3C). We changed positively charged residues in these loops into negatively charged residues, in various combinations, and we mutated two hydrophobic residues in the β5-β6 loop individually to aspartic acid. The positively charged residues do not correspond to the canonical $Ca2^+$ liganding residues in loops 1 and 3 required for the $Ca2^+$ dependent lipid-binding activity of C2 domains (Sutton et al., 1995; Sutton and Sprang, 1998), as they are absent in the C2 domain of auxilin. We also made two mutants with changes in the P loop of the phosphatase-like domain: His159 and Cys160 to Ala in one construct and Gly164 to Ala in the other. The mutations in the C2 domain all reduced binding to liposomes containing phosphoinositides but had no discernable effect on binding to liposomes that contained PC with PI or PS; the mutations in the P loop had little or no effect. We conclude that membrane affinity and possibly a contribution to head group specificity depend strongly on the C2-domain surface that includes the β1-β2 and β5-β6 loops (Figure 3A). The corresponding loops on one of the two C2 domains of synaptotagmin likewise appear to interact with a phosphoinositide-containing membrane (Bai et al., 2004). There is evidence that $Ca2^+$ binding induces a reorientation of domain C2B, causing its β1-β2 and β5-β6 loops to insert into the bilayer, but there is no indication that these loops participate in specific interactions with phosphoinositides. In auxilin, we

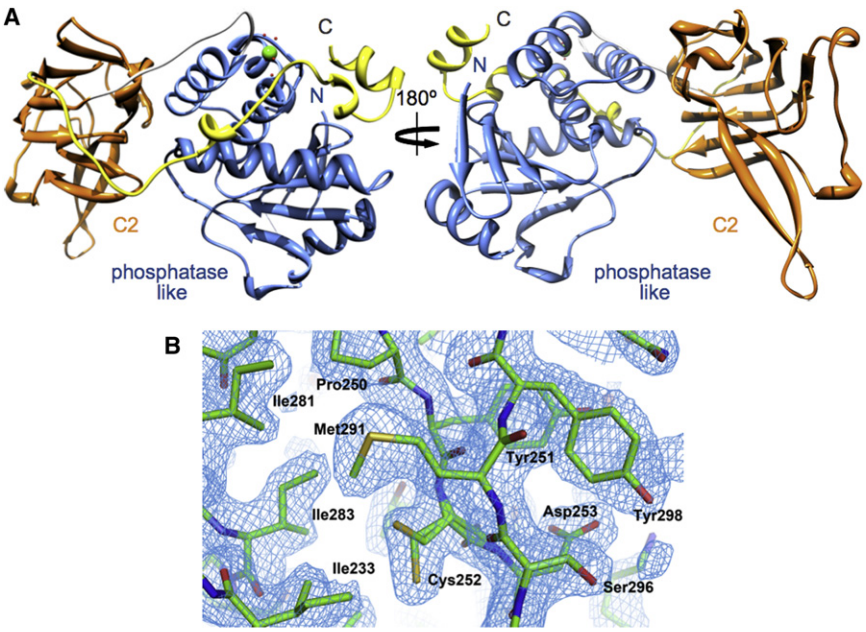

C

```
                                                                  pβ0
  1 mdssgasspd mepsyggglf dmvkggagrl fsnlkdnlkd tlkdtssrvi qsvtsytkgd

     pβ1        pβ2                    pα1         pβ3
 61 ldftyvtsri ivmsfpldsv digfrnqvdd irsfldsrhl dhytvynlsp ksyrtakfhs

    pβ4                    pα3              pβ5            pα4
121 rvsecswpir qapslhnlfa vcrnmynwll qnpknvcvvh cldgraassi lvgamfifcn

           pα5                    pα6                    cβ1
181 lystpgpavr llyakrpgig lspshrrylg ymcdlladkp yrphfkplti ksitvspvpf

                cβ2      cβ3                    cβ4         cβ5
241 fnkqrngcrp ycdvligetk iyttcadfer mkeyrvqdgk ifiplsitvq gdvvvsmyhl

                   cβ6                   cβ7                   cβ8
301 rstigsrlqa kvtntqifql qfhtgfipld ttvlkftkpe ldacdvpeky pqlfqvtldv

                                      pα7
361 elqphdkvme ltppwehyct kdvnpsilfs shqehqdtlv
```

Figure 2. Overall Structure of the PTEN-like Region of Auxilin 1

(A) Ribbon diagram showing the structure of auxilin 1 (40–400). The phosphatase-like region is in blue; the C2 domain, in orange. The views in A are related by a 180° rotation about the vertical axis. Figure made with Chimera.

(B) Representative example of the σA-weighed 2Fo-Fc electron density map, showing a region of the interface between the phosphatase-like and the C2-domain regions contoured at 1σ.

(C) Sequence of bovine auxilin 1 highlighting the elements of secondary structure; the nomenclature follows the description of PTEN (Lee et al., 1999).

expect that the phosphatase-like domain—and in particular, the region that corresponds to the PTEN catalytic cleft—is likely to be the principal specificity determinant. Definitive exploration of that region will require a more exhaustive mutational analysis. We have failed to obtain crystals with a short-chain phosphoinositide, which could guide choice of mutations. The published structure of PTEN does not have a bound substrate: a model for PTEN substrate binding is based on a tartrate from the crystallization medium at the active site of the enzyme (Lee et al., 1999).

Recruitment of Auxilin to Coated Pits

We tested the effects of the mutations just described on recruitment of auxilin to coated pits, using previously described live-cell imaging methods (Massol et al., 2006; Saffarian and Kirchhausen, 2008). In the earlier work, we had shown that auxilin appears in coated pits only after a burst of dynamin has led to release of the vesicle from the parent (plasma) membrane (Massol et al., 2006) (see also Lee et al., [2006]). In Figure 4A, we show as kymograph displays, the fluorescence from clathrin (labeled with a light-chain-mCherry chimera) and full-length auxilin (labeled with EGFP). The abrupt appearance of auxilin, just before uncoating (loss of the clathrin signal), is evident in Figure 4A (construct #1, Aux1 wt; wild-type control). Its absence is equally clear in Figure 4A, which shows the effect of one particular mutation (construct #3, Aux1 R301E/R307E/K311E) and confirms that deletion of the PTEN domain (construct #0, ΔPTEN Aux1) also eliminates recruitment (Lee et al., 2006; Massol et al., 2006). We note that in the case of the mutant auxilin, the clathrin still uncoats, as expression of the mutated, fluorescent auxilin does not eliminate recruitment of endogenous auxilin. Figure 4B compares the number of coated-pit associated auxilin spots in cells expressing wt auxilin and each of the mutants. The concordance of lipid-binding and recruitment is good, except for the R245E mutation (construct #16), which diminishes lipid binding but has no detectable effect on coated-pit association.

Model for Membrane Binding

The various C2-domain mutations that diminish membrane association in the experiments reported in Figure 3C are likely to map direct contacts with the lipid bilayer. The changes included charge reversal at several positively charged residues, which we propose will interact with negatively charged lipid head groups, and introduction of aspartic acid instead of hydrophobic residues at the tip of loop 3. Assuming that the catalytic cleft of the phosphatase-like domain also interacts with a lipid head group (presumably from a phosphoinositide), then only the orientation of the C2 and phosphatase-like domains shown in Figure 3A will allow all the relevant residues to face the membrane. Depending on how far loop 3 of the C2 domain

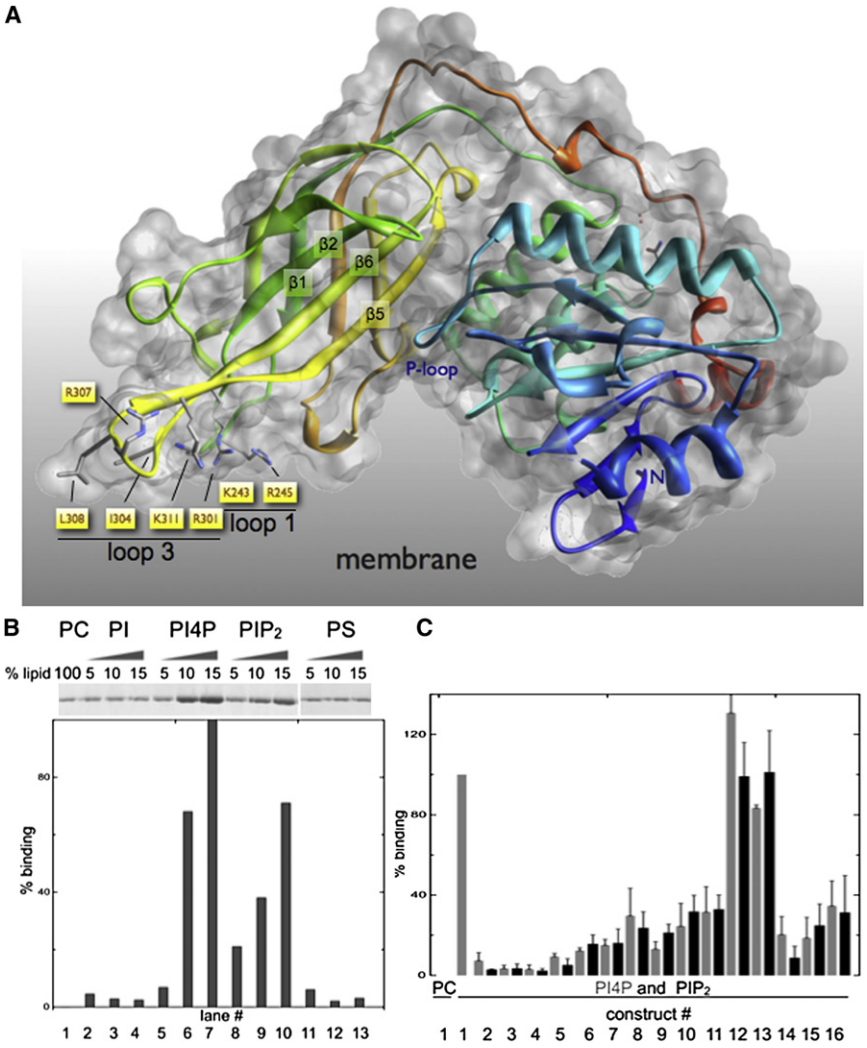

Figure 3. Interaction In Vitro of the Auxilin 1 PTEN-like Region with Specific Phosphoinositides

(A) Ribbon diagram of the PTEN-like region of auxilin showing the location of residues within the C2 region that we have mutated to test their role in lipid binding. The model is oriented to show the proposed orientation of this part of auxilin with respect to the cell membrane.

(B) The upper panel shows Coomassie blue staining after SDS-PAGE fractionation of wild-type PTEN-like region of auxilin 1 bound to liposomes containing either PC only or varying amounts (% w/w) of the indicated lipids. The bottom panel shows a bar plot comparing the average relative binding obtained from two independent experiments. To facilitate the comparison, the data were normalized to zero (binding to liposomes containing only PC) and 100% (binding to liposomes containing 15% PI4P).

(C) Bar plot comparing the relative binding (average ±SD) of wild-type and mutants forms of the PTEN-like region of auxilin to liposomes containing 85% and 15% PI4P. The results in each bar are from three independent experiments.

dips into the membrane (for example, whether the hydrophobic side chains at the tip of the loop penetrate as far as the proximal methylene groups of the fatty-acyl chains), it is possible that an inositol phosphate head group could be accommodated in the cleft of the phosphatase-like domain without displacing the phosphoinositide from its normal position within the bilayer. The C terminus of the entire fragment is positioned so that the polypeptide chain that follows could project away from the membrane and toward the clathrin coat. The 150 amino acid residues between the end of the PTEN-like region and the N terminus of the clathrin-binding region could easily span the ~100 Å gap between the location of the auxilin J-domain in a clathrin coat and its vesicle membrane. That segment is probably also quite extended in solution, as the Stokes radius of intact auxilin (62 Å) is much larger than expected for a 900 residue globular protein (Ahle and Ungewickell, 1990).

Potential Role of Specific Lipid Binding in Recruiting Auxilin to Newly Budded Coated Vesicles

The only reasonably abundant phosphoinositide in the plasma membrane is PI (4,5) P2 (about 0.5% of total lipid). Indeed, interaction with the head group of this lipid assists recruitment to the plasma membrane of proteins such as the AP-2 clathrin adaptor (Cremona et al., 1999; Gaidarov and Keen, 1999). As auxilin recruitment occurs only after a vesicle has separated from the bulk membrane (Lee et al., 2006; Massol et al., 2006), PI (4,5) P2 in unlikely to determine specific binding to the pinched-off vesicle. PI-4-P is a better candidate, as it could be produced from PI (4,5) P2 by an enzyme such as synaptojanin or similar lipid phosphatase recruited to the coated pit or to the coated vesicle (Perera et al., 2006). Even if that enzyme were present before membrane fission, the product would diffuse out of the bud and PI {4,5} P2 would maintain its equilibrium concentration. A vesicle 700 Å in diameter (about the size the vesicle within a typical endocytic clathrin coat containing 60–80 triskelions) would contain about 100 PI (4,5) P2 molecules, and even partial conversion to PI4P would recruit sufficient auxilin to drive uncoating (e.g., one auxilin per vertex). The strongest binding in the experiments in Figure 3 is indeed to liposomes with PI4P, a result that is in agreement with earlier observations using lipid-strips (Lee et al., 2006; Massol et al., 2006). A definitive conclusion will require both a more sensitive and quantitative assay and a structure with a suitable ligand.

EXPERIMENTAL PROCEDURES

cDNA Constructs and Protein Expression

We inserted the PTEN-like domain of bovine auxilin1 (residues 40–400) into the bacterial expression vector pGEX-KG by PCR amplification and restriction enzyme directed ligation. A tobacco etch virus (TEV) protease cleavage site was introduced in frame immediately after the thrombin site of the expression

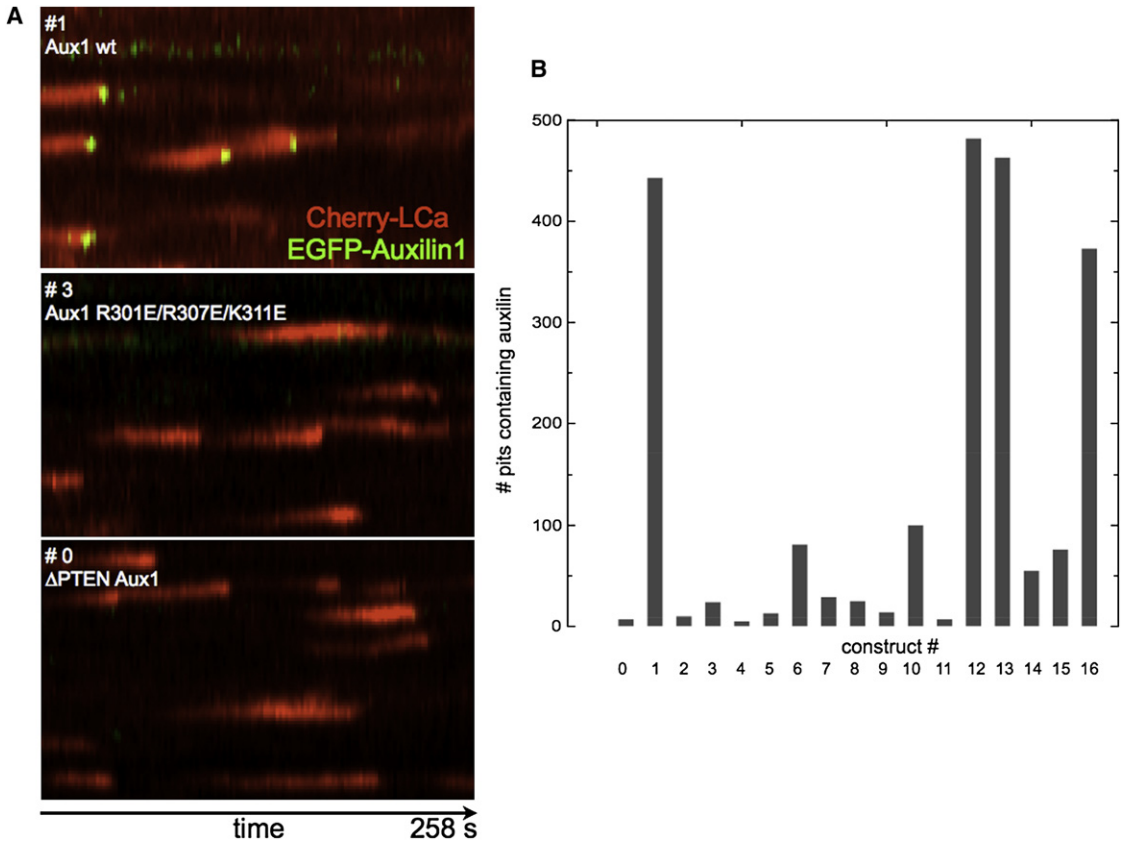

Figure 4. The PTEN-like Region of Auxilin Is Required for the Major Recruitment to Endocytic Clathrin-Coated Structures

(A) Live-cell imaging time series in TIRF illumination presented as kymograph views, with frames acquired every 1.6 s, from BSC1 monkey cells expressing a wild-type EGFP-auxilin 1 chimera (construct #1, Aux1 wt), an EGFP-auxilin1 mutant with three point mutations in its PTEN-like region (construct #3, Aux1 R301E/R307E/K311E), or a EGFP-auxilin 1 deletion mutant lacking the entire PTEN-like region (construct #0, ΔPTEN Aux1); a clathrin light chain LCa-cherry was coexpressed in each case. All constructs were expressed transiently for 20 hr. Selected examples are presented with equally normalized fluorescence intensities. (B) The bar plot compares the distribution of auxilin recruitment bursts in cells expressing EGFP chimeras of wild-type auxilin with the distribution in cells expressing mutants within the PTEN-like region of EGFP-auxilin. As shown previously (Massol et al., 2006), auxilin bursts are seen only in coated vesicles just after they have pinched off from the plasma membrane and just before disassembly.

vector and upstream of the auxilin insert. Mutations in this construct and in EGFP-Aux1 (Massol et al., 2006), the full-length bovine Auxilin1 (910 residues) inserted into the mammalian expression vector pEGFP-C1 (Clontech, Palo Alto, CA), were obtained using the QuickChange protocol (Stratagene). We verified by DNA sequencing the accuracy of all constructs.

Recombinant GST fusion proteins of wild-type and mutant forms of the PTEN-like domain of auxilin1 were expressed at room temperature (~22°C) in the presence 0.4 mM IPTG in *E. coli* BL21 (DE3) first grown at 37°C to an OD600 = 0.6–0.8. The cells from a 6 liter culture grown for 12 hr post IPTG induction were harvested by centrifugation at 4000 rpm for 20 min at 4°C in a JS 4.2 rotor (Beckman Coulter, Carlsbad, CA), and the pellets were resuspended in 125 ml buffer A (20 mM Tris [pH 7.0], 200 mM NaCl, 5 mM DTT) containing Roche protease inhibitor cocktail (Roche Applied Science, Indianapolis, IN). The samples were then frozen in liquid nitrogen and store at −80°C.

The frozen cells were thawed rapidly to room temperature in a water bath and lysed on ice by sonication (power set at 6; 10 cycles of 10 s on and 30 s off). Debris was removed by centrifugation for 30 min. at 4°C and 19,000 rpm in a Beckmann Ti 45 rotor. The supernatant was mixed with 9 ml of a 75% slurry of glutathione-Sepharose 4B beads (GE Healthcare) preequilibrated with 20 mM Tris (pH 7.0), 200 mM NaCl and incubated overnight at 4°C with continuous rotation. The beads were collected on a column and washed with 50 ml buffer A; then with 50 ml buffer A plus 1% Triton X-100; then twice with 50 ml buffer A and twice with 5 ml TEV buffer (50 mM Tris [pH 8.0], 100 mM NaCl, 5 mM DTT). The beads were then resuspended with 7 ml TEV buffer containing 100 μl recombinant TEV protease (~1 mg/ml) and incubated overnight at 4°C with constant rotation. The beads were repacked, and the released products recovered in the flow through and in a further elution with another 7 ml of TEV buffer. The pooled eluates were frozen in liquid nitrogen and stored at −80°C.

For further purification, the stored solutions were thawed to room temperature in a water bath, and the proteins were concentrated at 4°C to about 8 ml by ultra filtration in a 15 ml Amicon Ultra-15 Centrifugal Filter with Ultracel-10 membrane (10K Da molecular weight cutoff; Millipore, Billerica, MA). The concentrate was loaded onto a Superdex S200 26/60 gel filtration column (GE Healthcare) equilibrated in 20 mM Tris (pH 7.0), 200 mM NaCl, 1 mM DTT and run at a flow of 2 ml/min. The PTEN-like domain of auxilin1 elutes as a single species at the same position as chicken ovalbumin. Fractions containing the recombinant fragment were pooled, concentrated by ultra filtration to about 21.5 mg/ml in 20 mM MES (pH 6.0), 200 mM NaCl, and 1 mM TCEP (Tris (2-carboxyethyl) phosphine) and stored at −80°C. Monodispersity was confirmed by analytical ultracentrifugation.

Structure Determination

Crystals were obtained by hanging-drop vapor diffusion at 20°C by equilibrating a against 15.5% PEG 4000, 0.1 M HEPES (pH 7.5), 0.01 M $CaCl_2$, 0.8 M NaCl; the initial drop contained 1 μl of the sample and 1 μl of the well buffer. The crystals began to appear overnight and grew in 7 days to a final

size of ~0.05 × 0.05 × 0.3 mm^3. Harvested crystals were transferred to 15.5% PEG 4000, 0.1 M HEPES (pH 7.5), 0.01 M $CaCl_2$, 1 M NaCl, and 25% (v/v) glycerol and flash-frozen in liquid nitrogen. Diffraction data to a minimum Bragg spacing of 2.18 Å were collected at 100°K on the ID-24E beamline at the Advanced Photon Source (Argonne National Laboratory, Argonne, Il). The crystals, in space group P3221, a = b = 137.9 Å and c = 51.33 Å, contained one molecule per asymmetric unit. Data were processed and scaled in the HKL2000 program suite. Intensities from oscillation images (1°) were integrated with DENZO (Otwinowski, 1993); scaling and merging were carried out with SCALEPACK (Otwinowski, 1991). Subsequent computations used CCP4 programs (CCP4, 1994). The data were placed on an approximate absolute scale using TRUNCATE (CCP4). The statistics of the final data set are in Table 1.

The structure was determined by molecular replacement using Phaser. Nonconserved residues between the auxilin PTEN-like region and human PTEN were identified by sequence alignment using ClustalW. Initial model coordinates were obtained from the phosphatase subdomain of the human PTEN X-ray crystal structure (PDB entry 1D5R) with the nonconserved residues modified to alanine using Chainsaw (in CCP4) (Stein, 2008). Refinement of the model was carried out with Refmac5 (in CCP4), with a random subset of 5% of all the reflections set aside for cross validation and Rfree calculation. Manual adjustments to the models were carried out with Coot (Emsley and Cowtan, 2004). After the refinement of the protein part was completed, solvent molecules were added. The model has good stereochemistry, with 89.5% of residues in the most favored region of the Ramachandran plot and none in disallowed regions. Refinement statistics are presented in Table 1.

Liposome Binding Assay

Liposomes used for the binding assay contained at least 85% (w/w) phosphatidylcholine (PC) and up to 15% (w/w) of phosphatidylserine (PS), phosphatidylinositol (PI), phosphatidylinositol 4-phosphate, (PI4P), phosphatidylinositol-and (4,5)-bis-phosphate (PI (4,5) P2) (Avanti Polar Lipids, Inc., Alabaster, AL). To prepare liposomes, the appropriate lipid stock solutions in chloroform were mixed, evaporated under a gentle nitrogen gas stream, and dried overnight under vacuum. Liposomes were made at room temperature by vigorous vortex mixing for 1 min with 10 mM Tris (pH 7.5), 50 mM NaCl, 1 mM DTT to a final total lipid concentration of 1.25 mM.

The binding assay was performed for 25 min at room temperature using approximately 1 μM protein and 1 mM freshly prepared liposomes in a final volume of 125 μl; the incubated liposomes were centrifuged at 70,000 rpm (TLA-100 rotor; TL100 ultracentrifuge; Beckman Coulter, Inc, Brea, CA) for 10 min at 4°C. The supernatant was carefully removed, and the pellet fraction was subjected to SDS-12% PAGE analysis using Coomassie blue staining and gel densitometry. Data are reported as average of two independent experiments (Figure 3B) or as average ±SD of three independent experiments (Figure 3C).

Live-Cell Imaging

BSC1 monkey cells stably expressing rat brain LCa1-cherry were used in conjunction with transient expression of wild-type EGFP-auxilin1 or of selected mutants within its PTEN-like domain. Cells were used approximately 20 hr posttransfection with Lipofectamine (Invitrogen, Carlsbad, CA) as previously described (Massol et al., 2006). Cells expressing relatively low amounts of the fluorescent auxilin chimeras were selected for live-cell imaging using total internal reflection fluorescence (TIRF) microscopy (Saffarian and Kirchhausen, 2008). About 20,000–40,000 cells were plated on glass #1.5 coverslips (25 mm in diameter) 10 hr before the actual imaging experiment. Up to this point, the cells were grown at 37°C, in Dulbecco's Modified Eagle Medium (DMEM) supplemented with 10% fetal bovine serum and in the presence of humidified air and 5% CO_2. Cells were imaged in GIBCO's CO_2 independent medium in the absence of phenol red (Invitrogen) and in the presence of humidified air. The temperature of the sample holder (20/20 Technologies, Wilmington, NC) was kept at 37°C using a Peltier-controlled holding device. The holding device and the stage were surrounded by a custom-designed air-controlled environmental chamber kept at 33°C–35°C.

The TIRF imaging experiments were conducted as described (Massol et al., 2006; Saffarian and Kirchhausen, 2008) using a Marianas system controlled with SLIDEBOOK 4.2 (Intelligent Imaging Innovations, Denver, CO). The imaging system consists of an inverted 200M Zeiss microscope, a computer-controlled spherical aberration correction device, solid-state lasers exciting at 488 nm (Coherent, Santa Clara, CA) and 561 nm Cobolt, Solna Sweden), an acousto-optic tunable filter, a Dual-View unit (Photometrics, Tucson, AZ) equipped with a 565DCXR dichroic mirror and HQ525/40 and HQ620/50 emission filters (Chroma, Rockingham, VT) and a Quantum EMCCD camera (Photometrics, Tucson, AZ). Image sets were acquired every 1.6 s, each composed of sequential exposures at the two wavelengths of 50 ms in duration and separated by about 70 ms.

Object tracks selected for analysis corresponded to clathrin-coated pits according to criteria described previously (Ehrlich et al., 2004; Massol et al., 2006; Saffarian et al., 2009; Saffarian and Kirchhausen, 2008). Selected objects have the following characteristics: (a) they appear as diffraction-limited fluorescent spots; (b) they are present in both the first and last frames of the time series; (c) their centroid has moved less than two pixels (~200 nm) between consecutive time frames; (d) the tracks do not merge with or dissociate from nearby objects. We determined the extent of auxilin association with endocytic clathrin pits in the selected object tracks by counting the number of colocalization events within a projection of the time series into a single frame. As we have shown previously (Massol et al., 2006), auxilin spots appear as brief bursts just before loss of clathrin from the coated vesicle. In Figure 4, representative examples are shown as kymographs normalized for intensity of fluorescence.

ACCESSION NUMBERS

The coordinates have been deposited in the Brookhaven protein data bank, accession number 3N0A.

ACKNOWLEDGMENTS

We thank the staff of beamline 24ID-E at APS and members of our laboratories for support. We thank Emanuele Cocucci for help setting up the TIRF experiments and Eric Marino for technical support with the fluorescence microscopes. The work was funded in part by NIH grants GM36548 (T.K.) and U54 AI057159 (NERCE Imaging Resource) (T.K.). R.G. was an American Heart Association Postdoctoral Fellow and D.H. was a Helen Hay Whitney Postdoctoral Fellow. S.C.H. is an Investigator in the Howard Hughes Medical Institute.

Received: May 13, 2010
Revised: June 21, 2010
Accepted: June 22, 2010
Published: September 7, 2010

REFERENCES

Ahle, S., and Ungewickell, E. (1990). Auxilin, a newly identified clathrin-associated protein in coated vesicles from bovine brain. J. Cell Biol. *111*, 19–29.

Bai, J., Tucker, W.C., and Chapman, E.R. (2004). PIP2 increases the speed of response of synaptotagmin and steers its membrane-penetration activity toward the plasma membrane. Nat. Struct. Mol. Biol. *11*, 36–44.

Barouch, W., Prasad, K., Greene, L.E., and Eisenberg, E. (1994). ATPase activity associated with the uncoating of clathrin baskets by Hsp70. J. Biol. Chem. *269*, 28563–28568.

Brett, T.J., and Traub, L.M. (2006). Molecular structures of coat and coat-associated proteins: function follows form. Curr. Opin. Cell Biol. *18*, 395–406.

CCP4 (Collaborative Computational Project, Number 4).. (1994). The CCP4 Suite: Programs for Protein Crystallography. Acta Crystallogr. D Biol. Crystallogr. *50*, 760–763.

Cremona, O., Di Paolo, G., Wenk, M.R., Luthi, A., Kim, W.T., Takei, K., Daniell, L., Nemoto, Y., Shears, S.B., Flavell, R.A., et al. (1999). Essential role of phosphoinositide metabolism in synaptic vesicle recycling. Cell *99*, 179–188.

Ehrlich, M., Boll, W., Van Oijen, A., Hariharan, R., Chandran, K., Nibert, M.L., and Kirchhausen, T. (2004). Endocytosis by random initiation and stabilization of clathrin-coated pits. Cell *118*, 591–605.

Emsley, P., and Cowtan, K. (2004). Coot: model-building tools for molecular graphics. Acta Crystallogr. D Biol. Crystallogr. *60*, 2126–2132.

Fotin, A., Cheng, Y., Grigorieff, N., Walz, T., Harrison, S.C., and Kirchhausen, T. (2004). Structure of an auxilin-bound clathrin coat and its implications for the mechanism of uncoating. Nature *432*, 649–653.

Gaidarov, I., and Keen, J.H. (1999). Phosphoinositide-AP-2 interactions required for targeting to plasma membrane clathrin-coated pits. J. Cell Biol. *146*, 755–764.

Greene, L.E., and Eisenberg, E. (1990). Dissociation of clathrin from coated vesicles by the uncoating ATPase. J. Biol. Chem. *265*, 6682–6687.

Haynie, D.T., and Ponting, C.P. (1996). The N-terminal domains of tensin and auxilin are phosphatase homologues. Protein Sci. *5*, 2643–2646.

Holstein, S.E., Ungewickell, H., and Ungewickell, E. (1996). Mechanism of clathrin basket dissociation: separate functions of protein domains of the DnaJ homologue auxilin. J. Cell Biol. *135*, 925–937.

Kanaoka, Y., Kimura, S.H., Okazaki, I., Ikeda, M., and Nojima, H. (1997). GAK: a cyclin G associated kinase contains a tensin/auxilin-like domain. FEBS Lett. *402*, 73–80.

Kirchhausen, T. (2009). Imaging endocytic clathrin structures in living cells. Trends Cell Biol. *19*, 596–605.

Lee, J.O., Yang, H., Georgescu, M.M., Di Cristofano, A., Maehama, T., Shi, Y., Dixon, J.E., Pandolfi, P., and Pavletich, N.P. (1999). Crystal structure of the PTEN tumor suppressor: implications for its phosphoinositide phosphatase activity and membrane association. Cell *99*, 323–334.

Lee, D.W., Wu, X., Eisenberg, E., and Greene, L.E. (2006). Recruitment dynamics of GAK and auxilin to clathrin-coated pits during endocytosis. J. Cell Sci. *119*, 3502–3512.

Massol, R.H., Boll, W., Griffin, A.M., and Kirchhausen, T. (2006). A burst of auxilin recruitment determines the onset of clathrin-coated vesicle uncoating. Proc. Natl. Acad. Sci. USA *103*, 10265–10270.

Otwinowski, Z. (1991). Maximum likelihood refinement of heavy atom parameters. In Isomorphous Replacement and Anomalous Scattering, W. Wolf, P.R. Evans, and A.G.W. Leslie, eds. (Warrington, UK: Science and Engineering Council/Daresbury Laboratory), pp. 80–86.

Otwinowski, Z. (1993). Oscillation data reduction program. In Data Collection and Processing, L. Sawyer, N. Isaacs, and S. Bailey, eds. (Warrington, England: Science and Engineering Research Council/Daresbury Laboratory), pp. 56–62.

Perera, R.M., Zoncu, R., Lucast, L., De Camilli, P., and Toomre, D. (2006). Two synaptojanin 1 isoforms are recruited to clathrin-coated pits at different stages. Proc. Natl. Acad. Sci. USA *103*, 19332–19337.

Saffarian, S., and Kirchhausen, T. (2008). Differential evanescence nanometry: live-cell fluorescence measurements with 10-nm axial resolution on the plasma membrane. Biophys. J. *94*, 2333–2342.

Saffarian, S., Cocucci, E., and Kirchhausen, T. (2009). Distinct dynamics of endocytic clathrin-coated pits and coated plaques. PLoS Biol. *7*, e1000191.

Schmid, S.L., and Rothman, J.E. (1985). Enzymatic dissociation of clathrin cages in a two-stage process. J. Biol. Chem. *260*, 10044–10049.

Stein, N. (2008). CHAINSAW: a program for mutating pdb files used as templates in molecular replacement. J. Appl. Crystallogr. *41*, 641–643.

Sutton, R.B., and Sprang, S.R. (1998). Structure of the protein kinase Cbeta phospholipid-binding C2 domain complexed with Ca2+. Structure *6*, 1395–1405.

Sutton, R.B., Davletov, B.A., Berghuis, A.M., Sudhof, T.C., and Sprang, S.R. (1995). Structure of the first C2 domain of synaptotagmin I: a novel Ca2+/phospholipid-binding fold. Cell *80*, 929–938.

Ungewickell, E., Ungewickell, H., Holstein, S.E., Lindner, R., Prasad, K., Barouch, W., Martin, B., Greene, L.E., and Eisenberg, E. (1995). Role of auxilin in uncoating clathrin-coated vesicles. Nature *378*, 632–635.

Woscholski, R., Finan, P.M., Radley, E., Totty, N.F., Sterling, A.E., Hsuan, J.J., Waterfield, M.D., and Parker, P.J. (1997). Synaptojanin is the major constitutively active phosphatidylinositol-3,4,5-trisphosphate 5-phosphatase in rodent brain. J. Biol. Chem. *272*, 9625–9628.

